IJAME
Int. J. of Applied Mechanics and Engineering, 2026, vol.31, No.3, pp.115-129
DOI: 10.59441/ijame/223945

PARAMETRIC INVESTIGATION OF AN ASSESSED SUBCRITICAL DUAL-PRESSURE EVAPORATION ORGANIC RANKINE CYCLES BASED ON DIFFERENT HEAT SOURCE TEMPERATURES

O. Rowshanaie[1*], M.Z. Mohd Tohir[1] and H. Rowshanaie[2]
[1]Department of Chemical and Environmental Engineering, Universiti Putra Malaysia (UPM), MALAYSIA
[2]Department of Crop Science, Universiti Putra Malaysia (UPM), MALAYSIA
E-mail: omid.rowshanaie@gmail.com

The dual-pressure evaporation Organic Rankine Cycle (ORC) consists of two compression processes, two evaporation processes, and two expansion processes, and is becoming more prevalent than single-pressure evaporation ORCs due to its higher performance and maximum net power output. This study investigates different heat sources analysis in a simulated parametric dual-pressure evaporation ORC according to the assessment design process. The current dual-pressure evaporation ORC makes a comparison between R245fa, an old refrigerant, and R1233zd(E), a substitute for R245fa, as working fluids, paying attention to three water temperatures (100 , 125 , and $150\ ^{o}C$) as a heat source to generate maximum net power output. Based on designing an assessment process for dual-pressure evaporation ORC at $100^{o}C$ and $125^{o}C$ heat sources, R1233zd(E) is compared with R245fa, revealing an improvement of $9.58kW$ and $16.14kW$ in maximum net power output. Furthermore, according to the first and second laws of efficiency, R1233zd(E) exhibits improvements of 0.09% and 0.56% , as well as 0.15% and 1.04% , respectively. The pressure rise in low and high-pressure compression processes, parallel with a higher exergy flow rate in evaporation processes of R1233zd(E), demonstrates a direct and positive influence with a maximum net power output. At $150^{o}C$, the power generated by the lower-pressure turbine improved by $28.1\ kW$ in R1233zd(E) compared with R245fa.

Keywords: assessment process, dual-pressure evaporation Organic Rankine Cycle (ORC), maximum net power output, first and second law of efficiencies.

1. Introduction

Nowadays, the Organic Rankine Cycle (ORC), one of the most effective technologies for converting low- and medium-grade heat sources into power, is attracting interest in the chemical process industry (CPI). The ORC has numerous advantages, such as a simple structure, readily available components, and easy maintenance, which, along with its wide range of low boiling point refrigerant working fluids, leads to its prevalence worldwide [1-4].

Among a wide range of usable working fluids in ORC, R245fa from the hydrofluorocarbons (HFCs) is known as one of the most admired and high-performance working fluids in our era. The foremost environmental problems in selecting a suitable working fluid for ORC are the lowest Global Warming Potential (GWP) and zero Ozone Depletion Potential (ODP). For these critical environmental issues, the R1233zd(E) from hydrofluoroolefins (HFOs) with the lowest GWP and zero ODP is selected as the best replacement for R245fa and considered in ORC applications [5, 6].

The dual-pressure evaporation ORC, with applying two evaporation and compression processes compared with simple ORC, has some pivotal advantages consist including better temperature match between working fluid and heat source fluids during evaporation processes and lowest irreversibility loss. These parametric advantages cause to the generation of higher net power output and thermal efficiency from dual-pressure evaporation ORC [7-10]. Therefore, the dual-pressure evaporation ORC is evaluated by a few

* To whom correspondence should be addressed

scholars, including Li *et al.* [11] evaluated a dual-pressure evaporation ORC driven by nine refrigerant working fluids, especially R245fa and water as the heat source in $100-200°C$. Their results illustrate that, with increasing the heat source temperature, the net power output and system efficiency increase significantly. Also, the evaporation pressure with increasing the heat source temperature has a positive relationship. Furthermore, they achieved maximum net power output improvement for R245fa compared with other working fluids. Manente *et al.* [12] designed and examined a dual-pressure evaporation ORC by applying some effective refrigerant working fluids, especially R245fa, and investigating the effect of different temperatures of geothermal water as a heat source (100, 125, 150, 175 and $200°C$). The analyzed results revealed that, with enhanced geothermal water temperatures, the heat recovery efficiency, thermal efficiency, and system efficiency are improved dramatically. Likewise, among the refrigerant working fluids used in this designed dual-pressure evaporation ORC, R245fa demonstrated the highest performance. Li *et al.* [13] tried to consider a thermodynamic analysis on dual-pressure evaporation ORC by paying attention to the influence of 100, 125, 150 and $175°C$ of heated water as the main heat source on thermodynamic parameters with applying some refrigerant working fluids, which the main one was R245fa. They achieved, by increasing the heat source temperatures, the maximum net power output and thermal efficiency, showing the positive and direct impact with the highest amount for R245fa. Zheng *et al.* [14] measured the thermodynamic parameters on dual-pressure evaporation ORCs in different heat source temperatures (90, 100, 110 and $120°C$) by using R245fa and R152a. They found out that the maximum net power output and the second law of efficiency improved by increasing the heat source temperatures.

In this study, we designed and simulated an assessment process for a dual-pressure evaporation ORC to compare the effects of three different hot water temperatures (100, 125 and $150°C$) as a heat source. Also, R245fa and R1233zd(E) (as a substitution for R245fa) are applied. To evaluate pressure rise and turbine input viscosity during the low- and high-pressure compression processes of a dual-pressure evaporation ORC, the assessment focuses on improving the maximum net power output and the first- and second-law efficiencies.

2. Methodology

2.1. Theory of dual-pressure evaporation ORC

As illustrated in Fig.1, the current designed dual-pressure evaporation ORC includes low and high-pressure compressions, two evaporation processes, two expansion processes, and a condensation process.

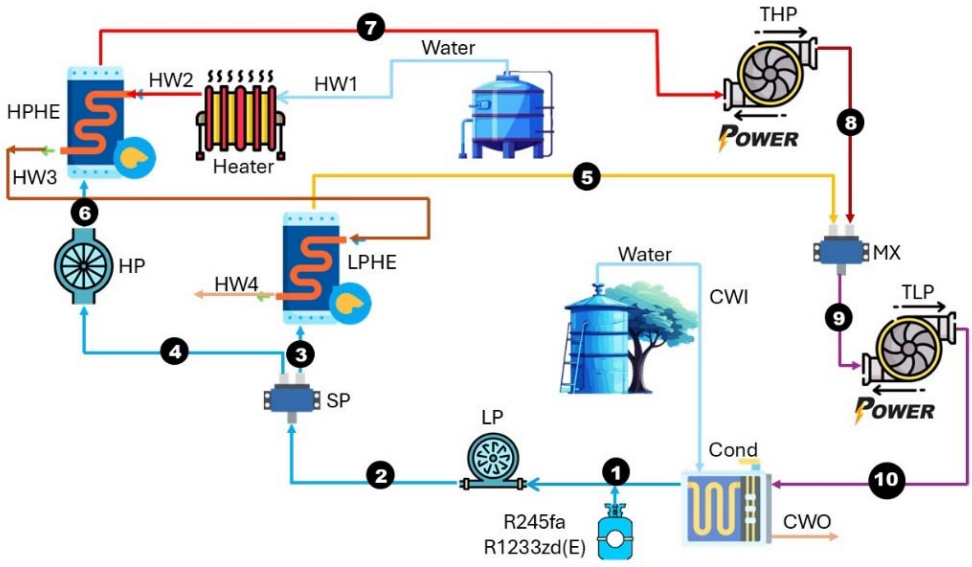


Fig.1. A theory schematic of the designed dual-pressure evaporation ORC.

According to this theory schematic of designed dual-pressure evaporation ORC, first of all, the pure working fluid (R245fa and R1233zd(E)) in minimum working conditions enters into the low-pressure pump as the first stage of compression pressure, and then by a splitter it is divided into the two fluids. One of them enters the low-pressure evaporator, and the second fluid flows into a high-pressure pump to convert it into the highest pressure, and then enters the high-pressure evaporator to complete the evaporation process. The low and high-pressure evaporation processes driven by standard water that convert into the hot water (*100* , *125* and *150°C*) by a conventional heater, and it is applied as a heat source for evaporation processes. At last, the high-pressure and evaporated refrigerant working fluid first flows into the high-pressure turbine to generate power, and second, after being mixed with the low-pressure output flow of the low-pressure evaporation process, enters the low-pressure turbine to generate the second stage of power, and this cycle is completed.

2.2. Simulation software

This study utilizes a robust simulation software, AspenPlus (V12), which is a chemical engineering simulation software for modeling, simulating, and evaluating the configuration of the dual-pressure evaporation ORC system. Likewise, the present organic refrigerant working fluids are calculated by the Peng-Robinson equation of state method. It is noted that this powerful simulation software leads to decreased operational costs at the real level in the industry and, in parallel, causes a reduction and prevents the number of system errors by increasing the safety of each section of the current study at implementation.

2.3. Thermophysical properties of selected refrigerant working fluids

As presented in Tab.1, R245fa, an old and high-performance working fluid, compared with R1233zd(E) as environmentally friendly working fluids, has a higher lifetime in the atmosphere and global warming potential (GWP) [5].

Table 1. Thermophysical properties of working fluids.

Working fluid	R245fa	R1233zd(E)
Structural formula	$C_3H_3F_5$	$C_3Cl\ H_2F_3$
Critical temperature/ ℃	*154.05*	*165.60*
Critical pressure/ bar	*36.40*	*35.70*
Molecular weight	*134.05*	*130.50*
Type	Dry	Dry
ASHREA safety classification	B1	A1
Flammability	Non flammable	Non flammable
Toxicity	Non toxic	Non toxic
ODP	*0*	*0.00034*
GWP	*1030*	*7*
Atmospheric life time/ year	*7.7*	*0.07*

2.4. Assessment process of simulated dual-pressure evaporation ORC

The primary input parameters, assumptions, constraints, and boundary conditions used during the simulation of the dual-pressure evaporation ORC assessment process have already been added and are presented in Tab.2.

Table 2. Initial input parameters, assumptions, constraints, and boundary conditions.

Input Data	Value
Initial mass flow rate of working fluid at low-pressure pump $[kg/h]$	*200,000*
Vapor fraction of working fluid at input of low-pressure pump	*0*
The minimum temperature approach at low and high pressures of evaporators and condenser $[°C]$	*10*
The mass flow rate of hot water and cooling water $[kg/h]$	*500,000*
The operating temperature of water inputted into the heater $[°C]$	*25*
The operating pressure of water inputted into the heater $[Bar]$	*1*
The operating temperature of hot water $[°C]$	*100*, *125* and *150*
The operating pressure of hot water $[Bar]$	*1*
The operating temperature of cooling water $[°C]$	*25*
The operating pressure of cooling water $[Bar]$	*1*
The isentropic efficiency at low and high pressures of pumps and turbines $[\%]$	*85*
The mechanical efficiency at low and high pressures of pumps and turbines $[\%]$	*85*
The heat loss in all pipelines, low and high pressures of evaporators and condenser	Neglected
Pressure drop in low and high pressures of evaporators and condenser	No
Temperature cross detected in low and high pressures of evaporators and condenser	No
Chemical loss from the ORC	No

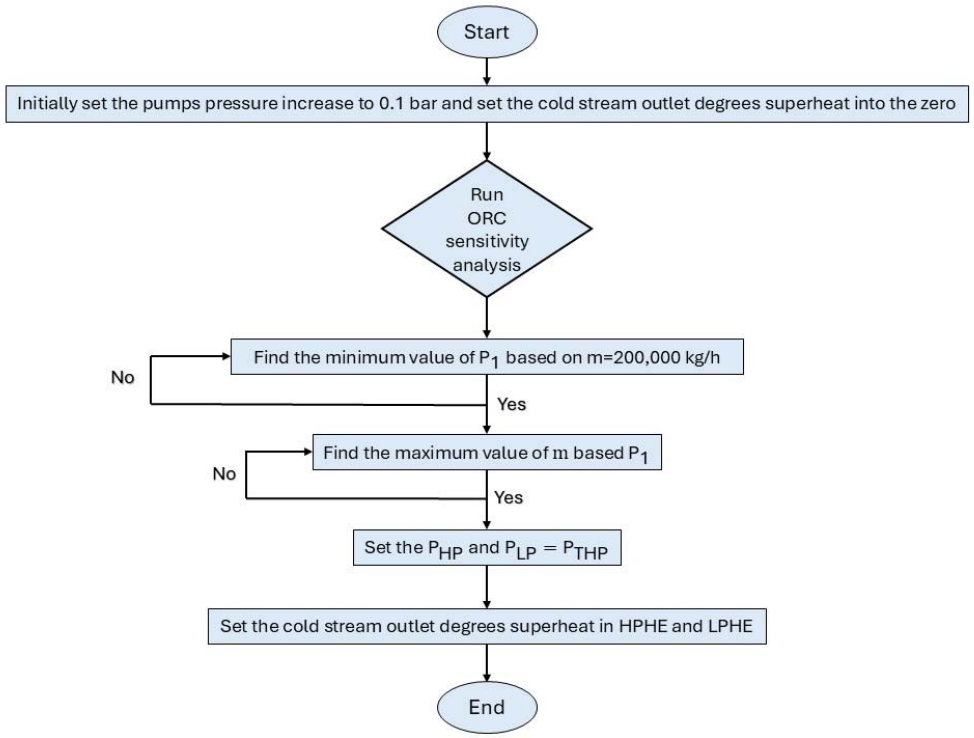


Fig.2. An assessment process of the designed and simulated dual-pressure evaporation ORC.

As illustrated in Fig.2, the assessment process of designed and simulated dual-pressure evaporation ORC based on simulated schematic of Fig.3, is started by initially preparing the ORC with setting the mass flow rate to $200{,}000\ kg/h$, low and high pressures of pumps into only $0.1\ Bar$ pressure increases, turbines pressures to only $0.1\ Bar$ decreases, and at last set the cold stream outlet temperatures of evaporators to $0°C$. Then, tries to find the minimum value of P_1, and after setting it to the minimum amount, it tries to find and set the highest amount of mass flow rate of working fluid by using the sensitivity analysis of AspenPlus. After that, find and set the high and low pressures of compression processes, and finally achieve and set the cold stream temperature increases in the two evaporators separately.

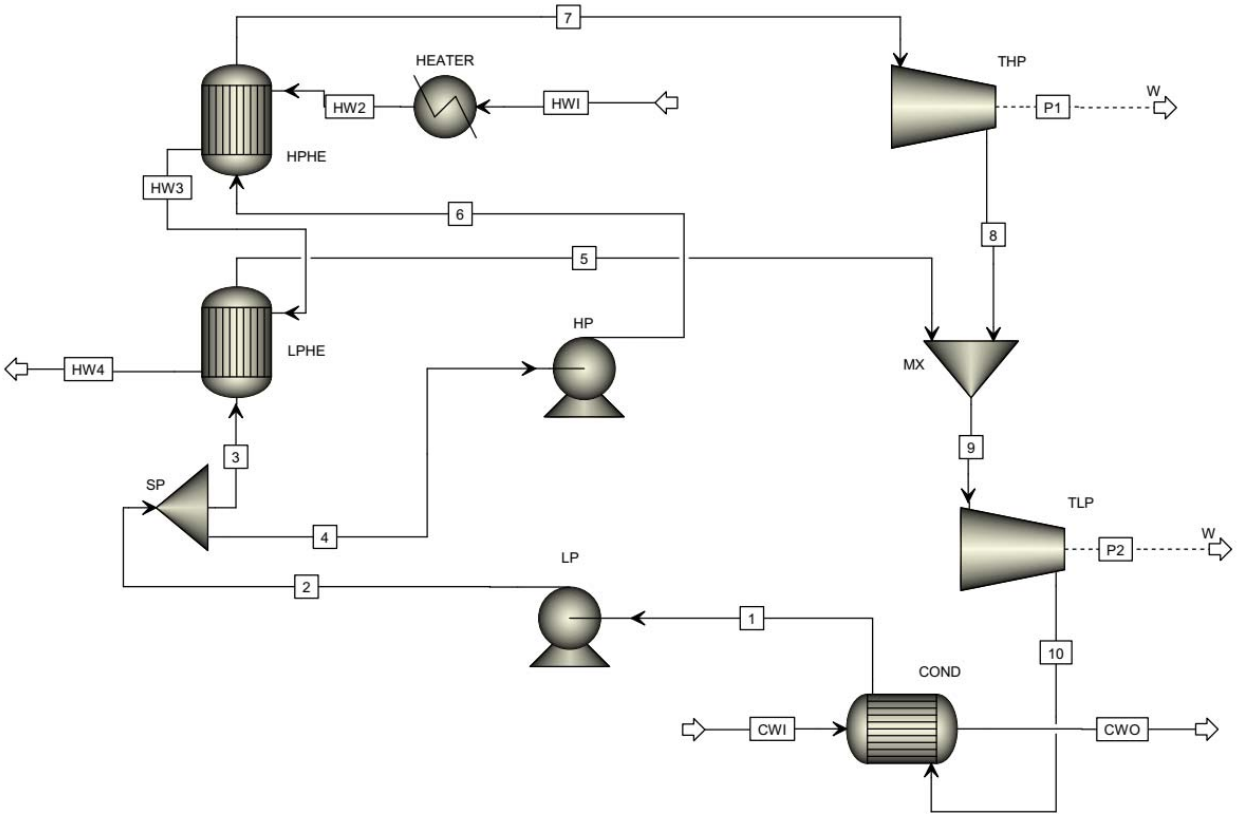


Fig.3. Simulated schematic of dual-pressure evaporation ORC.

As illustrated in Fig.4, the T-S diagram of this simulated assessed dual-pressure evaporation ORC has 2 stages: low pressure and high pressure. The working fluid under subcritical conditions is compressed by a low-pressure pump from a saturated liquid into the subcooled condition (1-2,3 as a compression process), then heated up to saturated and superheated vapor by a low-pressure evaporation process in the low-pressure evaporator (3-5 as a low-pressure evaporation process), and next, the working fluid flows into the mixer. Before this section, the divided working fluid from splitter, high compressed by high-pressure pump (4-6 as a high compression process) and then flow into the high-pressure evaporator (6-7 as a high-pressure evaporation process, which driven by three different temperatures of hot water, 100, 125, and $150\ °C$) and after that it flows into the high-pressure turbine (7-8 as an first expansion process) to generate power as work, after this section, the expanded working fluids (state point 8) mixed with low-pressure evaporation working fluid (state point 5) to expanded during low-pressure turbine to generate second stage of power (9-10 as an second expansion process). Finally, the exhausted working fluid is cooled to a saturated liquid in a condenser through a condensation process (10-1 as a condensation process) by using cooling water as a heat sink, thereby completing and continuing the dual-pressure evaporation ORC process.

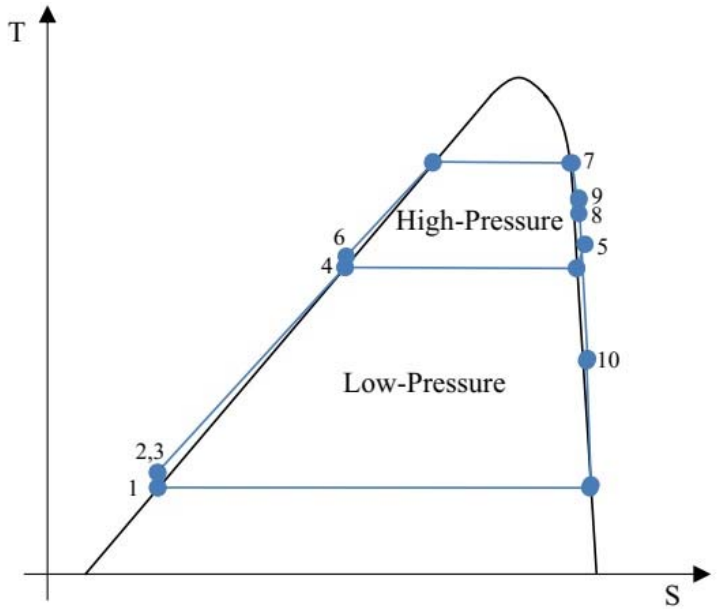


Fig.4. Temperature-entropy (T-S) diagram of dual-pressure evaporation ORC.

To clarify the current dual-pressure evaporation ORC system analysis, the following general assumptions are made:

- Simplifying the complexity of the model.
- Steady-state operating of the ORC system.
- Neglecting heat and pressure loss in heat exchangers and pipes.
- Friction pressure drop is neglected in pipelines and heat exchangers.
- Neglecting the influence of gravitational potential energy and fluid kinetic.
- No chemical loss from ORC.

2.5. The thermodynamic equations of the dual-pressure evaporation ORC system

2.5.1. Net power output

The power output generated from the low and high pressure of turbines (W_{TLP} and W_{THP}) is calculated by AspenPlus (V12); therefore, they can be calculated as follows:

$$W_{TLP} = \dot{m}_{wf}(h_9 - h_{10}), \tag{2.1}$$

$$W_{THP} = \dot{m}_{wf}(h_7 - h_8), \tag{2.2}$$

where $\dot{m}_{wf}$ is the mass flow rate of working fluid, h_9 and h_{10} are the input and output enthalpies of the low-pressure expansion process. Also, h_7 and h_8 are the input and output enthalpies of the high-pressure expansion process.

Likewise, the power consumed by the low and high pressure of pumps (W_{TLP} and W_{THP}) are calculated by AspenPlus (V12), so they can be calculated as follows:

$$W_{PLP} = \dot{m}_{wf}(h_2 - h_1), \tag{2.3}$$

$$W_{PHP} = \dot{m}_{wf}(h_6 - h_4), \tag{2.4}$$

here h_1 and h_2 are the input and output enthalpies of the low-pressure compression process. And, h_4 and h_6 are the input and output enthalpies of the high-pressure compression process.

The net power output, W_{net} generated by the dual-pressure evaporation ORC system, as the main objective function is as follows:

$$W_{net} = (W_{TLP} + W_{THP}) - (W_{PLP} + W_{PHP}). \tag{2.5}$$

2.5.2. Thermal efficiency of SORC system

The heat duty in low and high pressure evaporators (Q_{LPHE} and Q_{HPHE}) is calculated by AspenPlus (V12); therefore, they can be calculated as follows:

$$Q_{LPHE} = \dot{m}_{HW}(h_{HW3} - h_{HW4}), \tag{2.6}$$

$$Q_{HPHE} = \dot{m}_{HW}(h_{HW2} - h_{HW3}), \tag{2.7}$$

where $\dot{m}_{HW}$ is the mass flow rate of hot water, h_{HW2}, h_{HW3} and h_{HW4} are the input and output enthalpies of hot water during low and high pressure evaporation processes.

The dual-pressure evaporation ORC thermal efficiency, based on the first law of thermodynamics, is as follows:

$$\eta_{I,ORC} = \frac{W_{net}}{(Q_{LPHE} + Q_{HPHE})}. \tag{2.8}$$

Based on the first law of thermodynamics, the energy conversion efficiency is evaluated based on the quantity of energy converted in thermodynamic cycles. However, the second law analysis considered the thermal energy potential as a quality of energy for generating work. In this matter, exergy is defined as the maximum work at the specific temperature and pressure in a process stream, determined in an equilibrium condition between those specific temperature and pressure and the environment reference temperature (T_0) and pressure (P_0), as the change in the stream is reversible. Also, it is directly related to the enthalpy and entropy of the process stream.

$$Ex = h - T_0 s, \tag{2.9}$$

where h is the enthalpy stream, and s is the entropy stream in reference environment condition, $T_0 = 25°C$ and $P_0 = 1bar$.

The exergy stream is affected by temperature, pressure, and the fluid's composition. The exergy changes from state 1 to state 2 are as follows:

$$Ex_{1\text{-}2} = Ex_2 - Ex_1 = (h_2 - h_1) - T_0(s_2 - s_1). \tag{2.10}$$

Hence, the exergy difference in low and high pressure of evaporators (ΔE_{LPHE} and ΔE_{HPHE}) is calculated by AspenPlus (V12); therefore, the exergy difference during evaporation processes (ΔE_{EVAPs}) can be calculated as follows:

$$\Delta E_{LPHE} = Ex_5 - Ex_3 , \tag{2.11}$$

$$\Delta E_{HPHE} = Ex_7 - Ex_6 , \tag{2.12}$$

$$\Delta E_{EVAPs} = \Delta E_{LPHE} + \Delta E_{HPHE} . \tag{2.13}$$

here Ex_5 and Ex_3 are the exergy flow in the output and input of the assure evaporator. Ex_6 and Ex_7 represent the exergy flows at the input and output of the low-pressure evaporator.Finally, the dual-pressure evaporation ORC thermal efficiency, based on the second law of thermodynamics, is as follows:

$$\eta_{2,ORC} = \frac{W_{net}}{\Delta E_{EVAPs}} . \tag{2.14}$$

3. Results and discussion

3.1. Validation

To validate and verify the current ORC system under subcritical working conditions, an attempt is made to simulate the experimental ORC system $(250\ kW)$ [15].

Table 3. Verification and validation of the simulation results of the present ORC with other Ref. [15].

Parameter	Simulation	Ref. [15]	Difference (%)
Heat transfer rate of evaporation $[kW]$	*2619.46*	*2573*	*1.79*
Thermal efficiency of ORC $[\%]$	*8.33*	*9.5*	*13.12*
Net power output of ORC $[kW]$	*218.29*	*243*	*10.71*

The evidence from this validation, as shown in Table 3, reveals that the simulation model is accurate enough in terms of heat transfer rate of evaporation, thermal efficiency of the ORC, and net power output of the ORC, thereby validating it for further investigations, which guarantees the accuracy of this study.

3.2. The maximum net work (power) output

As shown in Fig.5, a comparison is performed between three different heat source temperatures, *100*, *125*, and *150 °C*, in R245fa and R1233zd(E) to investigate the maximum net power output from this simulated assessed dual-pressure evaporation ORC. According to Fig.5, based on the designed assessment process, at *100* and *125 °C* of heat source, R1233zd(E) compares with R245fa reveals the improvement in maximum net power output with *9.58 kW* and *16.14 kW* increase, respectively, because of lower viscosity and lower pump power consumption. But, at *150 °C*, the R245fa shows the better maximum net power output generated, because of higher high-pressure turbine power generated compared with R1233zd(E) (Fig.6) and better temperature match between R245fa and hot water during the high-pressure evaporation process. These results are in agreement with [11, 13].

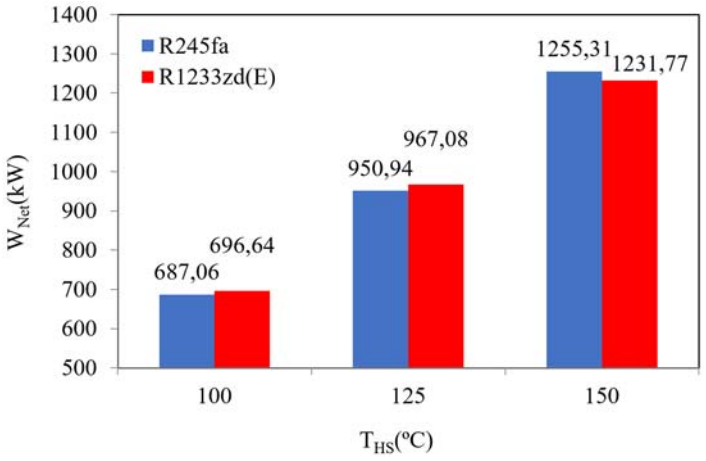


Fig.5. The maximum net power output generated by dual-pressure evaporation ORC for each working fluid at *100* , *125* , and *150* °*C* of heat source temperatures.

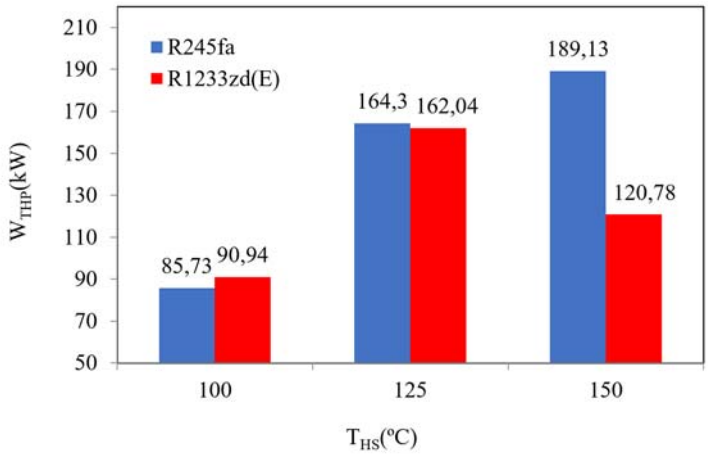


Fig.6. The high-pressure turbine power output generated by dual-pressure evaporation ORC for each working fluid at *100* , *125* , and *150* °*C* of heat source temperatures.

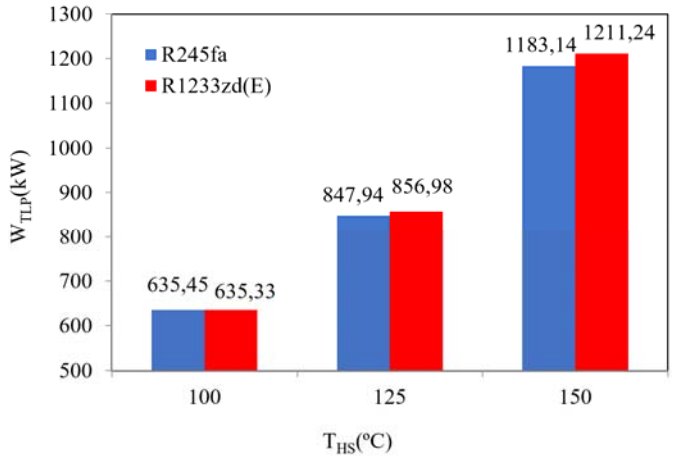


Fig.7. The low-pressure turbine power output generated by dual-pressure evaporation ORC for each working fluid at *100* , *125* , and *150* °*C* of heat source temperatures.

Figures 6 and 7 illustrate the influence of 100, 125, and $150\ ^{\circ}C$ of hot water as a heat source between R245fa and R1233zd(E) to evaluate the high and low pressure of turbines' power generated, respectively. These results in turbine high-pressure power generated demonstrate that the R1233zd(E) shows $5.21\ kW$ improvement compared with R245fa in $100^{\circ}C$ of hot water. In the results of low-pressure turbine power generated during the dual-pressure evaporation ORC based on the assessment process, the R1233zd(E) reveals $28.10\ kW$ power generated improvement compare with R245fa in the highest temperature of hot water, because of higher increases in heat duty of low-pressure evaporator and as a result in high-pressure of evaporator, which show the better temperature match during evaporation processes.

Figures 8 and 9 belong to the power consumption of high and low-pressure pumps in this assessed dual-pressure evaporation ORC. These results present the assessment process in all three temperatures of heat source success to achieve the lower power consumption for R1233zd(E) in both high and low-pressure pumps.

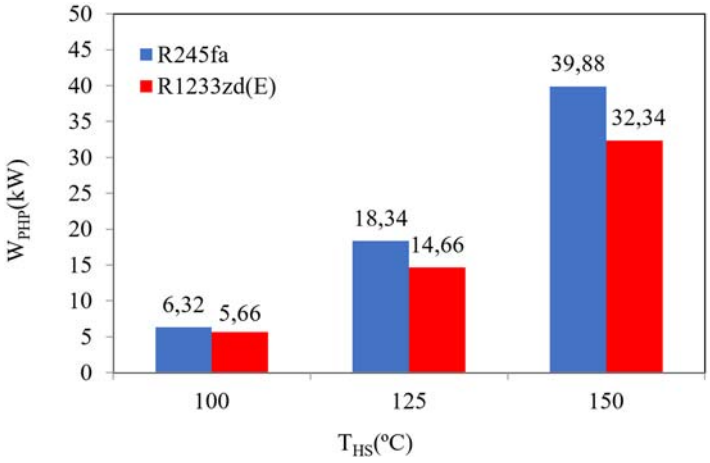


Fig.8. The high-pressure pump power output consumed by dual-pressure evaporation ORC for each working fluid at 100, 125, and $150\ ^{\circ}C$ of heat source temperatures.

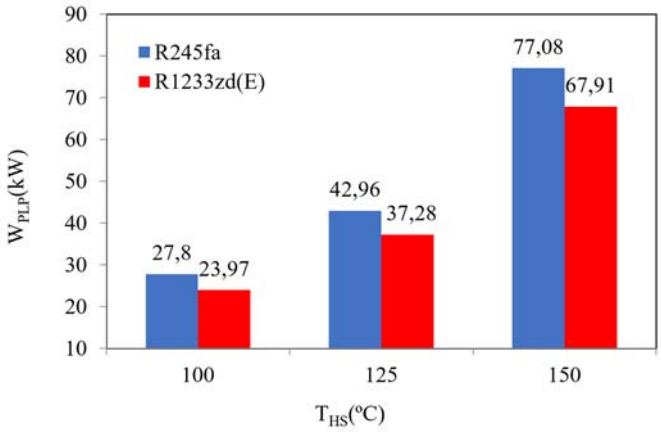


Fig.9. The low-pressure pump power output consumed by dual-pressure evaporation ORC for each working fluid at 100, 125, and $150\ ^{\circ}C$ of heat source temperatures.

According to Fig.10, during the assessment process, the pressure rise of R1233zd(E) shows lower increases compared with R245fa. As a result, it depicts the lower heat duty in evaporators. In contrast to Figures 11 and 12, the lower viscosity of R1233zd(E) compared with R245fa shows the lower heat loss. It has a positive effect to generate a higher net power output for R1233zd(E), especially at $125^{\circ}C$ of hot water.

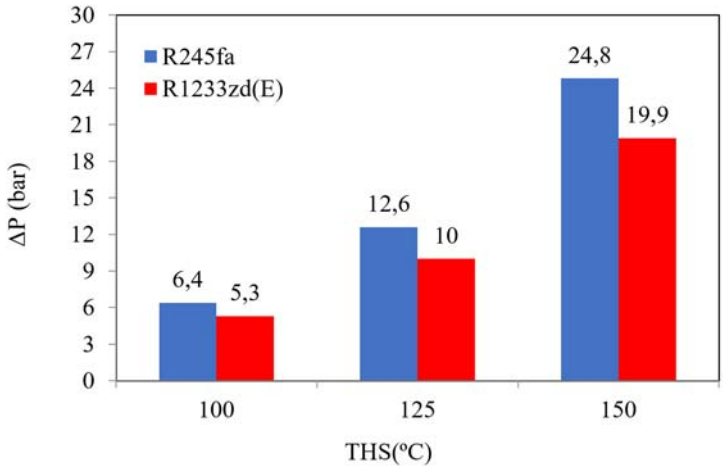


Fig.10. The pressure rise for each working fluid at 100, 125, and $150\ ^{\circ}C$ of heat source temperatures.

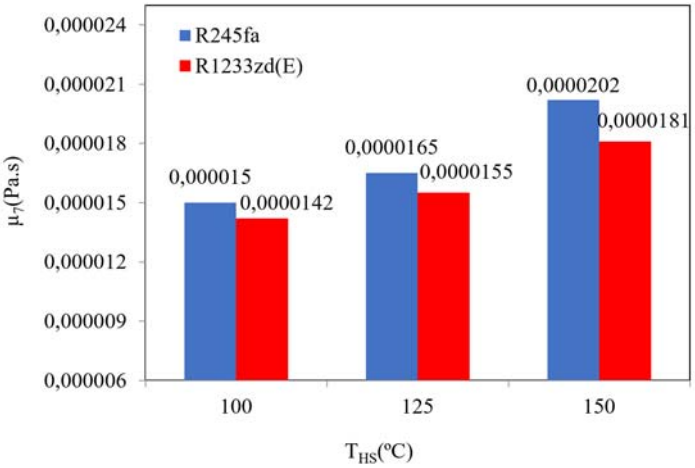


Fig.11. The high-pressure turbine input viscosity for each working fluid at 100, 125, and $150\ ^{\circ}C$ of heat source temperatures.

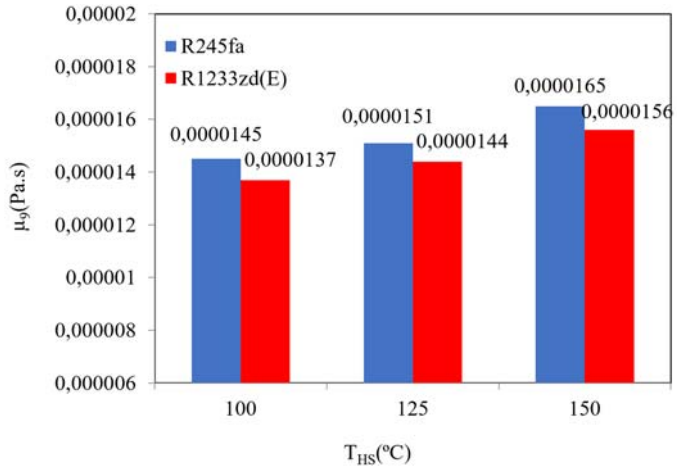


Fig.12. The low-pressure turbine input viscosity for each working fluid at 100, 125, and $150\ ^{\circ}C$ of heat source temperatures.

3.3. The first and second laws of dual-pressure evaporation ORC efficiencies

The foremost thermodynamic performance parameters are the first and second laws of efficiency. In both efficiencies, the net power output plays the key role to increase them, but the overall heat duty of high- and low-pressure evaporation ORC for the first law of efficiency, and in parallel the exergy differences in evaporation processes for the second law of efficiency have an adverse effect on them.

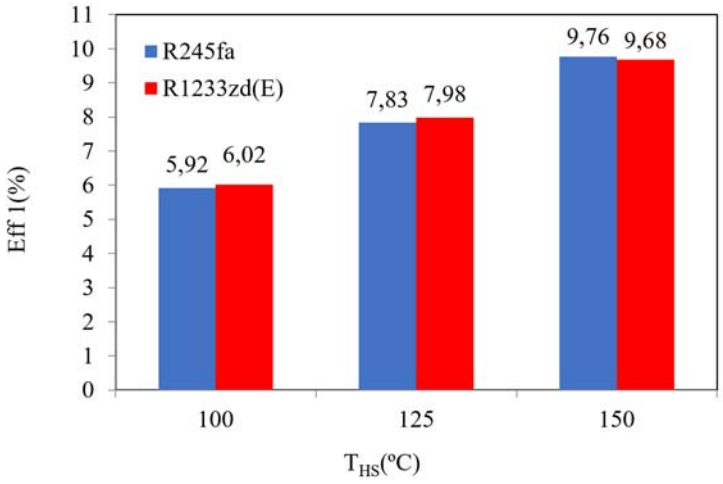


Fig.13. The first law of dual-pressure evaporation ORC thermal efficiency for each working fluid at *100*, *125*, and *150* °*C* of heat source temperatures.

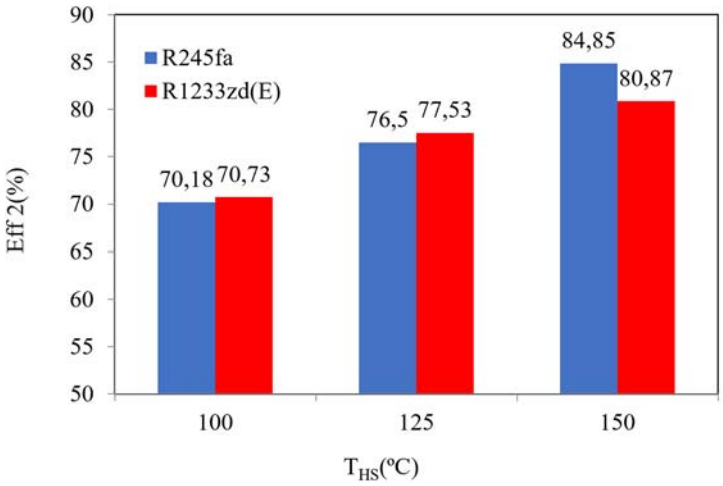


Fig.14. The second law of dual-pressure evaporation ORC thermal efficiency for each working fluid at *100*, *125*, and *150* °*C* of heat source temperatures.

According to Fig.13, which belongs to the first law of efficiency in the dual-pressure evaporation ORC at all three temperatures of hot water, the net power output has a pivotal effect on the first law of efficiency. So, based on the assessment process, at *100* and *125*°*C*, the R1233zd(E) shows the *0.10*% and *0.15*% improvement, respectively. Also, in these two temperatures of hot water, the R1233zd(E) illustrates the *0.55*% and *1.03*% improvement, respectively, compared with R245fa (Fig.14). These results are similar to those reported in [12, 14].

4. Conclusion

All in all, this study focused on designing and simulating an assessment process on a dual-pressure evaporation ORC driven by R245fa as an old but high performance and R1233zd(E) as a substitution with low GWP and lifetime in the atmosphere by make a comparison between 100, 125, and $150\ ^{\circ}C$ of hot water as the heat source and evaluate the effect of these different heat source temperatures on primary thermodynamic parameters in this application.

- Evaluating the maximum net power output of a simulated and assessed dual-pressure evaporation ORC demonstrates that the R1233zd(E) in 100, and $125°C$ of hot water temperatures has an improvement compared with R245fa. The main reason comes back to the lower viscosity and the lower pump's power consumption.

- Investigating the first and second laws of efficiencies and their results show the better achievement in 100, and $125°C$ of hot water for R1233zd(E) regarding higher maximum net power output. Furthermore, in the second law of efficiency, the higher exergy flow differences during evaporation processes have a positive effect for R1233zd(E).

As a recommendation for further research, utilize the EES (Engineering Equation Solver) method to enhance computational efficiency as a numerical simulation process, considering this study.

Author contributions

Omid Rowshanaie and Mohd Zahirasri Mohd Tohir initiated the literature collection, study design, simulation, validation, data collection, data analysis, draft paper writing, and revision. Hooman Rowshanaie reviewed the literature, drew the figures, and revised the manuscript. All authors read and approved the final manuscript.

Conflicts of interest

The authors declare no conflict of interest.

Nomenclature

$COND$ – condenser
CPI – chemical process industry
CW – cooling water
E – evaporator
Ex – exergy flow $[kW]$
GWP – global warming potential
h – enthalpy $\left[\frac{kJ}{kg}\right]$
HE – heat exchanger
HP – high-pressure
HW – hot water
in – input
LP – low-pressure
$\dot{m}$ – mass flow rate $\left[\frac{kg}{hr}\right]$
ODP – ozone depletion potential
ORC – organic Rankine cycle

P – pressure $[bar]$, pump
Q – heat duty $[kW]$
s – entropy $\left[kj.kg^{-1}.K\right]$
T – temperature $[°C]$, turbine
W – work (power) output $[kW]$
wf – working fluid
Δ – difference
η – efficiency $[\%]$
μ – viscosity $[Pa.s]$
0 – environment
$1-10$ – state points of T-S diagram

References

[1] Li B., Xie H., Sun L., Gao T., Xia E., Liu B., Wang J. and Long X. (2025): *Advanced exergy analysis and multi-objective optimization of dual-loop ORC utilizing LNG cold energy and geothermal energy*.– Renewable Energy, vol.239, No.122164, pp.1-14. https://doi.org/10.1016/j.renene.2024.122164.

[2] Hu X., Ma T., Dong Sh., Zhang Ch., Zhuang W. and Zhang T. (2025): *Design and selection of working fluids for ORC system using computer-aided molecular design and group contribution method*.– Applied Thermal Engineering, vol.274, No.126593, pp.1-19. https://doi.org/10.1016/j.applthermaleng.2025.126593.

[3] Zahedi R. and Ahmadi A. (2025): *Thermodynamic and thermoeconomic analysis of solar derived ORC with storage system utilizing PCM*.– Case Studies in Thermal Engineering, vol.68, No.105942, pp.1-16. https://doi.org/10.1016/j.csite.2025.105942.

[4] Feng Y.-Q., Wang Zh.-X., Xu K.-J., Yang Zh.-Zh., Liu M.-Y., Wu H.-J., Wang Y.-Zh. and He Zh.-X. (2025): *Data-driven multi-objective optimization of surfactant-modified nano-organic working fluids for enhanced heat transfer in ORC phase-change processes*.– Energy Conversion and Management, vol.333, No.119815, pp.1-21. https://doi.org/10.1016/j.enconman.2025.119815.

[5] Eyerer S, Wieland Ch, Vandersickel A and Spliethoff H (2016): *Experimental study of an ORC (Organic Rankine Cycle) and analysis of R1233zd-E as a drop-in replacement for R245fa for low temperature heat utilization*.– Energy, vol.103, pp.660-671. https://doi.org/10.1016/j.energy.2016.03.034

[6] Eyerer S., Dawo F., Kaindl J., Wieland Ch. and Spliethoff H. (2019): *Experimental investigation of modern ORC working fluids R1224yd(Z) and R1233zd(E) as replacements for R245fa*.– Applied Energy, vol.240, pp.946-963. https://doi.org/10.1016/j.apenergy.2019.02.086.

[7] Li J., Peng X., Yang Zh., Hu Sh. and Duan Y. (2022): *Design, improvements and applications of dual-pressure evaporation organic Rankine cycles: A review*.– Applied Energy, vol.311, No.118609, pp.1-24. https://doi.org/10.1016/j.apenergy.2022.118609.

[8] Li J., Ge Zh., Liu Q., Duan Y. and Yang Zh. (2018): *Thermo-economic performance analyses and comparison of two turbine layouts for organic Rankine cycles with dual-pressure evaporation*.– Energy Conversion and Management, vol.164, pp.603-614. https://doi.org/10.1016/j.enconman.2018.03.029.

[9] Wang M., Zhang J., Zhao S., Liu Q., Zhao Y. and Wu H. (2019): *Performance investigation of transcritical and dual-pressure Organic Rankine Cycles from the aspect of thermal match*.– Energy Conversion and Management, vol.197, No.111850, pp.1-17. https://doi.org/10.1016/j.enconman.2019.111850.

[10] Li J., Ge Zh., Duan Y. and Yang Zh. (2019): *Effects of heat source temperature and mixture composition on the combined superiority of dual-pressure evaporation organic Rankine cycle and zeotropic mixtures*.– Energy, vol.174, pp.436-449. https://doi.org/10.1016/j.energy.2019.02.186.

[11] Li J., Ge Zh., Duan Y., Yang Zh. and Liu Q. (2018): *Parametric optimization and thermodynamic performance comparison of single-pressure and dual-pressure evaporation organic Rankine cycles*.– Applied Energy, vol.217, pp.409-421. https://doi.org/10.1016/j.apenergy.2018.02.096.

[12] Manente G., Lazzaretto A. and Bonamico E. (2017): *Design guidelines for the choice between single and dual pressure layouts in organic Rankine cycle (ORC) systems*.– Energy, vol.123, pp.413-431. https://doi.org/10.1016/j.energy.2017.01.151.

[13] Li D., He Zh., Wang Q., Wang X., Wu W. and Xing Z. (2021): *Thermodynamic analysis and optimization of a partial evaporating dual-pressure organic Rankine cycle system for low-grade heat recovery*.– Applied Thermal Engineering, vol.185, No.116363, pp.1-16. https://doi.org/10.1016/j.applthermaleng.2020.116363.

[14] Zheng Zh., Cao J., Wu W. and Leung M.K.H. (2022): *Parallel and in-series arrangements of zeotropic dual-pressure Organic Rankine Cycle (ORC) for low-grade waste heat recovery*.– Energy Reports, vol.8, pp.2630-2645. https://doi.org/10.1016/j.egyr.2022.01.057.

[15] Fu B.-R., Lee Y.-R. and Hsieh J.-Ch. (2015): *Design, construction, and preliminary results of a 250-kW organic Rankine cycle system*.– App. Thermal Eng., vol.80, pp.239-346. https://doi.org/10.1016/j.applthermaleng.2015.01.077.

Received: September 9, 2025
Revised: June 2, 2026